

# Kinetics of diffuesion-controlled oxygen ordering in a lattic-gas model of YBa2Cu3O7-

**Andersen, Jørgen Vitting; Bohr, Henrik; Mouritsen, Ole G.**

*Published in:*
Physical Review B

*Link to article, DOI:*
10.1103/PhysRevB.42.283

*Publication date:*
1990

*Document Version*
Publisher's PDF, also known as Version of record

# Kinetics of diffusion-controlled oxygen ordering in a lattice-gas model of $YBa_2Cu_3O_{7-\delta}$

Jørgen Vitting Andersen
*Department of Structural Properties of Materials, The Technical University of Denmark, Building 307, DK-2800 Lyngby, Denmark*

Henrik Bohr
*Risø National Laboratory, DK-4000 Roskilde, Denmark*

Ole G. Mouritsen
*Department of Structural Properties of Materials, The Technical University of Denmark, Building 307, DK-2800 Lyngby, Denmark*

(Received 28 March 1990)

Nonequilibrium properties of oxygen ordering in high-$T_c$ superconductors of the Y-Ba-Cu-O type are studied via computer simulation of an anisotropic two-dimensional lattice-gas model in which the ordering processes are controlled by diffusion across the sample edges. With a view to designing optimal annealing strategies, various quenches and annealing schedules through the phase diagram are investigated. The ordering kinetics and the grain morphology are found to have a characteristic dependence on the thermal treatment of the system.

It is well established experimentally that the ordering of oxygen in the CuO basal planes of ceramic high-$T_c$ superconductors of the type $YBa_2Cu_3O_{7-\delta}$ plays an important role for the physical properties of the superconducting as well as normal states of these materials.[1-14] A particularly important issue is the lateral heterogeneity in the oxygen density[4-9] in the plane and how this heterogeneity is controlled by in and out diffusion of oxygen, by the grain structure of the ceramics, and by the structural metastability due to nonequilibrium conditions enforced by the thermal treatment of the material. While the detailed relationship is not well understood, it has been shown that there is a significant correlation between the superconductivity and the oxygen-vacancy ordering in the CuO planes.[2,4,5,7,11] A number of phases with different kinds of oxygen ordering have been identified,[1,11,13] notably an oxygen-deficient ($\delta \sim 1$) tetragonal phase which is semiconducting, an orthorhombic "single-cell" structure ($\delta \sim 0$, ortho-I) and an orthorhombic "double-cell" structure ($\delta \sim \frac{1}{2}$, ortho-II). The orthorhombic phases are superconducting and the superconducting transition takes place at about 60 K and 90 K, respectively, in the ortho-II and ortho-I phases.

Experimentally it is very difficult to distinguish between thermodynamically stable and metastable or mixed inhomogeneous states for these ceramics. Furthermore, the production parameters used are completely empirical. It is therefore important for the production of samples with desirable superconducting properties to be able to optimize the annealing and quenching schedules used in the experimental preparation procedures. The key variables in such schedules are the temperature and the ambient partial oxygen pressure. Theoretically[15-29] the properties of the oxygen ordering have been studied using a variety of theoretical approaches including the use of lattice-gas models.[16-18,20-29] Some of these models lead to phase diagrams with phases in accordance with the experimental observations, in addition to a host of other low-temperature phases[19,20,27,28] which arise due to the presence of competing interactions. Although some nonequilibrium properties have been studied theoretically[19,22,24] the major effort so far has been concerned with the static properties.

In the present paper we present a theoretical model study of the nonequilibrium oxygen ordering in the CuO planes, which explicitly takes into account the fact that the oxygen concentration varies during quenching and annealing and that the ordering processes and the resulting nonequilibrium structures are controlled by oxygen diffusion across the edges of a finite two-dimensional system. This finite system may be considered as an individual crystalline grain of the ceramic material in which the grain boundaries constitute the oxygen reservoir.[7] Hence the model explicitly incorporates the experimental fact[12] that oxygen diffusion predominantly takes place within the individual CuO planes and not between the planes. The oxygen atoms are assumed to occupy the sites of the regular lattice shown in Fig. 1(a). For the interactions between the oxygen atoms we have adopted the locally anisotropic lattice-gas model proposed by Wille *et al.*[18] The Hamiltonian of this model is given by

$$\mathcal{H} = -V_1 \sum_{i,j}^{\mathrm{NN}} n_i n_j - V_2 \sum_{i,j}^{\mathrm{NNN(Cu)}} n_i n_j - V_3 \sum_{i,j}^{\mathrm{NNN}} n_i n_j + \mu \sum_{i \in \mathrm{E}} n_i , \tag{1}$$

where $n_i = 0, 1$ is an occupation variable and $V_1$ is the nearest-neighbor (NN) interaction strength. Interactions between a pair of oxygen atoms at next-nearest-neighbor

 

(NNN) sites are given by $V_2$ or $V_3$ depending on whether or not the pair is bridged by a Cu atom. In our implementation, the model is defined on a finite square lattice of $L \times L$ sites with open boundaries. The oxygen concentration in the lattice is controlled kinetically by a chemical potential, $\mu$, which acts only at the edges ($E$) of the lattice. By employment of a kinetic principle, which corresponds to Glauber dynamics at these edges and Kawasaki (particle-vacancy) exchange dynamics in the interior of the lattice, this chemical potential maintains in equilibrium a certain homogenous oxygen concentration throughout the interior. The chemical potential simulates the partial oxygen pressure of the environment. The fact that $\mu$ is only applied at the edges, together with the kinetic principle employed, ensures that oxygen atoms can only enter or leave the system via diffusion across the edges. Therefore, $\mu$ only occurs in the transition probabilities for oxygen atoms which move between the edge and the interior of the lattice. The chemical potential simply acts as a particle pump of strength $\mu$ corresponding to the gain in energy for a particle which diffuses from the edge (and hence the particle bath) into the lattice. The statistical ensemble corresponding to this kinetic lattice model is that of a hybrid of a grand-canonical and a canonical ensemble. A similar ensemble was recently used to study steady-state properties of a diffusive system driven by a chemical-potential gradient.[30] Below we report on equilibrium and nonequilibrium properties of this kinetic lattice model as obtained by Metropolis Monte Carlo computer-simulation techniques.

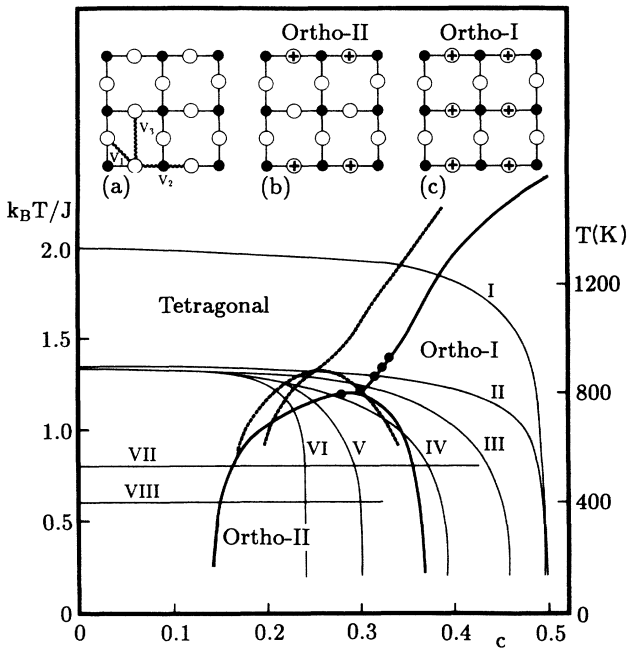


FIG. 1. Phase diagram (in heavy solid lines) for the lattice-gas model of oxygen ordering in $YBa_2Cu_3O_{7-\delta}$ with $c = (1-\delta)/2$. (a) Lattice model of the CuO basal plane. Sites available for O atoms are indicated by ○ and Cu atoms are indicated by •. (b) and (c) represent schematically the ground-state oxygen ordering in the ortho-II and ortho-I phases where the occupied sites of oxygen are denoted by ⊕ corresponding to densities $c = \frac{1}{4}$ and $\frac{1}{2}$, respectively. The various quenches and annealing schedules studied in this work are indicated by thin solid lines with an enumeration referred to in the text. The cooling rates for the various schedules are (in reduced units) I: 0.0001; II: 0.000 05; III: 0.0001; IV: 0.0002; V–VIII: 0.0001. The corresponding chemical potentials, $\mu/J$, are I–IV, VII–VIII: 5; V: 1; VI: 0. The right-hand axis is calibrated to absolute temperature by use of the data from Specht *et al.* (Ref. 14) as indicated by the symbols •. The dashed lines indicate the phase diagram obtained from cluster-variational-method calculations (Ref. 25).

In accordance with a recent theoretical study by Berera and de Fontaine[25] we have chosen the interaction constants of Eq. (1) as $V_1 < 0$, $V_2/V_1 = -0.75$, and $V_3/V_1 = 0.50$ corresponding to nearest-neighbor repulsion, and next-nearest-neighbor attraction across a Cu atom, and next-nearest-neighbor repulsion otherwise. For this choice of parameters we have determined by equilibrium Monte Carlo calculations the equilibrium phase diagram as shown in Fig. 1. The oxygen concentration in this diagram, $c = \langle n_i \rangle$, is related to the composition index of the stoichiometric formula as $c = (1-\delta)/2$. The phase diagram contains three one-phase regions, which we interpret as the tetragonal phase (oxygen-disordered) and the two orthorhombic (oxygen-ordered) phases. The ortho-I phase is a twofold degenerate ($2 \times 2$) structure and the ortho-II phase is a fourfold degenerate ($4 \times 1$) structure as shown in Figs. 1(b) and 1(c). The phase diagram contains a multicritical point. All phase lines of the diagram correspond to continuous transitions and the diagram is similar to that obtained from Monte Carlo and exact transfer-matrix calculations for slightly different parameter values.[26,29] In contrast, our mean-field calculations for the present model predict a diagram with first-order lines below the multicritical point and hence phase coexistence regions between the tetragonal and the ortho-II phases and between the ortho-II and ortho-I phases. Cluster-variational-method calculations, although quantitatively more reliable than the mean-field calculations, also predict incorrectly first-order transitions between the tetragonal and ortho-II phases,[25] cf. Fig. 1.

The nonequilibrium properties of the model are described in terms of a time parameter, $t$, which, when measured in units of Monte Carlo steps per site (MCS/s), refers to the stochastic dynamics of the underlying Metropolis scheme. There is no simple relation between this time and real physical time. The results to be reported below for the kinetic and time-dependent properties of the model should therefore only be compared qualitatively to experiments. The temperature of the heat bath with which the system interacts is taken to be of function of time, $T(t)$, associated with some characteristic cooling rate $v(t) = dT(t)/dt$. For the present model the cooling rate is given in reduced units of $k_BT[J(\mathrm{MCS/s})]^{-1}$. We shall here only be concerned with infinitely rapid cooling [i.e., $v(t) \to \infty$] and with constant cooling rates.[31] A few cases of heating and upwards quenching have also been investigated. When deal-

ing with nonequilibrium phenomena controlled by diffusion across the boundary of a finite system the size of the system becomes of obvious importance for the times involved. We have verified that the properties observed in systems of different linear dimensions $L$ to a rather high-accuracy scale with time according to $t \sim \sqrt{L}$ as expected for diffusion. Hence, the results reported below for certain selected system sizes can immediately be carried over to systems of other sizes. We are now going to report the results for a series of characteristic nonequilibrium paths through the phase diagram in Fig. 1. Each path is determined by three parameters, the initial (homogeneous) oxygen density, $c_o$ (in most cases chosen as $c_o = 0$), the oxygen gas pressure chemical potential, $\mu$, and the cooling schedule, $T(t)$. The system properties along the path are calculated as averages over a large number (typically 20–100) of independent paths described by the same parameters. These properties include the density $c(t)$, the dynamic structure factor $S(q,t)$, calculated as an average over the two canonical directions of the oxygen site lattice, and the length-distribution function, $P(R,t)$, for CuO chains, where $R$ is the chain length in units of the lattice parameter of the oxygen lattice. Furthermore, the evolution of selected microscopic configurations is monitored.

In the discussion of the evolution of the oxygen ordering and the transient inhomogeneous states it is important to realize that these states are determined by local stability conditions, which in turn involve the local density. Hence, structures may be formed which are not the equilibrium structures characterized by the particular global density. The general qualitative observation made from inspection of the microconfigurations is that in quenches from $c_o \simeq 0$ towards the oxygen-ordered phases of the phase diagram the system evolves through a series of characteristic inhomogeneous structures. For high $\mu$ and not too high $T$, the influx of oxygen firstly stabilizes a mantle of ortho-I structure, which may have a grain structure due to the double degeneracy. This mantle is more pronounced the larger $\mu$ is. Then this mantle dissolves by diffusion towards the interior of the system leading to a lower density and hence a stabilization of the ortho-II structure (which has the lower interaction energy) which eventually forms a core of the system. This core has a grainy structure due to the fourfold degeneracy. Hence the picture emerges of an inhomogeneous transient structure, cf. inset (b) of Fig. 2, with a mantle of the ortho-I phase and a core of the ortho-II phase. This structure and its morphology is fundamentally different from that obtained in model simulations which either assume fixed global concentration of oxygen[22,24] or allows for oxygen incorporation everywhere in the system. Such mixed ortho-I and ortho-II states are very frequent, and they occur everywhere in the region of the phase diagram where ortho-II is the equilibrium structure, cf. Fig. 1. These circumstances make it very difficult and demanding to determine the equilibrium phase diagram by simulation techniques.[26,29]

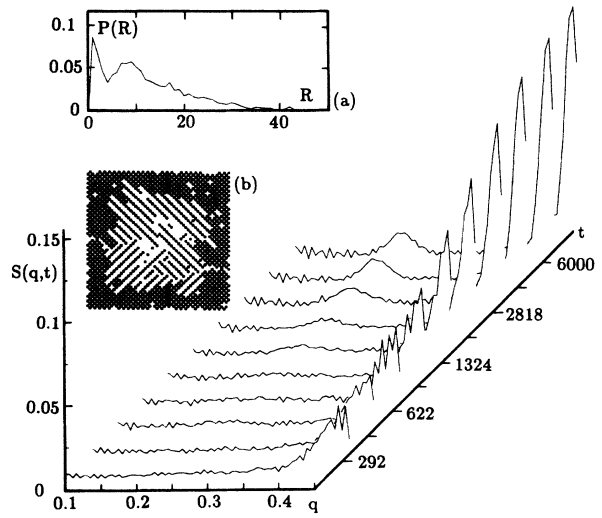


FIG. 2. Dynamical structure factor, $S(q,t)$, for quenches of type IV, cf. Fig. 1, given at different times $t$ (in units of MCS/s) on a logarithmic scale. The chemical potential is $\mu/J = 5$. The cooling rate is 0.0002 in reduced units. The length-distribution function, $P(R,t)$, for CuO chains is given in the inset (a) for $t = 6000$ MCS/s. The inset (b) shows a schematic picture of a microconfiguration typical of $t$ =2818 MCS/s. The data refer to a lattice with 60×60 sites.

A quantitative description of the kinetics of the ordering processes is given in terms of the time evolution of the dynamical structure factor, $S(q,t)$, and the CuO-chain length-distribution function, $P(R,t)$. We have performed a series of quenches through the phase diagram partly represented by the selection of paths indicated in Fig. 1. These paths are given by plotting the relation between $T(t)$ and the calculated nonequilibrium global density $c(t)$. Hence, states along these paths do not represent the corresponding points in the equilibrium phase diagram. The general systematics emerging from all these paths may be described as follows with reference to the roman numerals in Fig. 1.

*I: High-T, high-$\mu$ quenches.* Complete formation and annealing of the ortho-I phase with grain boundaries which disappear according to the usual curvature-driven Lifshitz-Allen-Cahn growth law for a nonconserved system is shown. There is no nucleation of the ortho-II phase and the CuO chains extend throughout the system. The results are only a little sensitive to the cooling rate.

*II–IV: Intermediate-T, high-$\mu$ quenches.* The initial temperature is in the region of the multicritical point. Slow cooling, $v = 0.000\,05$, leads to the same states as I, although the ordering process is somewhat slower. As the cooling rate is increased, going from II to IV, $v$ =0.0001 and 0.0002, cf. Fig. 2, a progressive amount of the ortho-II phase is nucleated and becomes trapped in the core of the system. This is illustrated in inset (b) of Fig. 2. Once this core has formed, it anneals extremely slowly and eventually becomes effectively frozen in. At the same time the average CuO-chain length decreases

as the cooling rate is increased. The length-distribution function, $P(R,t)$, at late times is also shown in Fig. 2(a) in the case of slow cooling $v = 0.0001$ from which it appears that in the frozen state the average chain length is about 10–20 lattice spacings. If the temperature is sufficiently below the multicritical point, e.g., $k_BT/J = 1.1$, even a slow cooling rate leads to entrapment of the ortho-II phase.

*V: Intermediate-T, intermediate-$\mu$ quenches.* The ortho-II phase is dominant with some element of the ortho-I phase occurring not as a mantle but rather in the grain boundaries of the different domains of the ortho-II phase. The average CuO-chain length is rather small, below 10 lattice spacings. The grain structure appears to be frozen in at low temperatures due to the accumulated excess density of oxygen trapped in the domain walls. The Bragg peak at $q = \frac{1}{4}$ does not diminish as time lapses.

*VI: Intermediate-T, low-$\mu$ quenches.* Only the ortho-II phase is formed, cf. Fig. 3. [Note that the $(4 \times 1)$ phase gives a Bragg peak at $q = \frac{1}{2}$ as well as at $q = \frac{1}{4}$.] The growth of the domains is persistent, however slow, and there is no excess oxygen in the domain boundaries to impede the growth.

*VII-VIII: Low-T, high-$\mu$ quenches.* The temperature is fixed. Formation of mixed phases with a core of ortho-II within a mantle of ortho-I phase occurs. The lower the temperature, the slower the formation of the core phase due to the necessity of crossing an activation barrier for detaching oxygen from the mantle before diffusion into the interior.

*Thermal cycling.* By rapidly heating the system back into the tetragonal phase, e.g., after a quench of type VI, it is possible to increase the oxygen content in the final state after a subsequent annealing to the same final temperature.

The major conclusion to be drawn from the above observations is that thermal treatments of our model of oxygen ordering in most cases result in transient nonequilibrium states. These states and their morphology are extremely sensitive to the annealing schedules employed. In particular it appears that for the production and the annealing of the oxygen-rich ortho-I phase it is important to choose an annealing schedule which avoids going below the equilibrium multicritical point. If the initial temperature is close to the multicritical point the cooling rate has to be low in order to enhance the content of the ortho-I phase. Hence the equilibrium phase diagram may be of some use for optimizing material properties, despite the fact that neither the model nor the real systems it may correspond to attain the equilibrium state within the observation time. Moreover, our simulations show that the

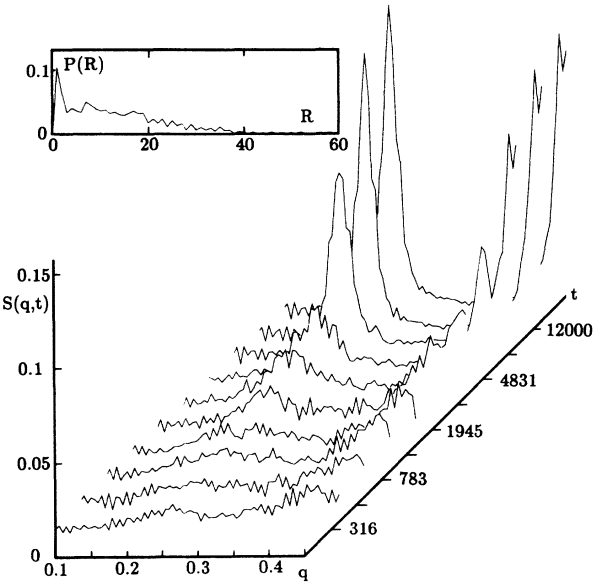


FIG. 3. Dynamical structure factor, $S(q,t)$, for quenches of type VI, cf. Fig. 1, with $\mu/J = 0$. Data are given for a series of times $t$ (in units of MCS/s), on a logarithmic scale. The inset shows the length-distribution function, $P(R,t)$, for CuO chains at $t = 12\,000$ MCS/s. The cooling rate is 0.0001 in reduced units. The data refer to a lattice with $60 \times 60$ sites.

time-limiting factor in the annealing of structures, which contain an amount of the ortho-II phase, is the accumulation of a local excess of oxygen in the domain boundaries. This leads to impediment of the growth, as observed in other phase-separation and impurity-controlled domain-growth problems.[32,33]

In conclusion we have studied by Monte Carlo simulation the nonequilibrium properties of a simple lattice-gas model of oxygen ordering in the CuO basal planes of high-$T_c$ superconductors of the Y-Ba-Cu-O type. By only permitting influx and outflux of oxygen across the edges of the system the model seeks to mimic the experimental conditions for the manufacturing of this type of material. Our study leads to a set of qualitative guidelines for the choice of optimal annealing schedules in which the equilibrium phase diagram plays an important role. Future refinements of modeling along these lines will involve a more detailed account of the different diffusion characteristics at the edges and in the interior, as well as a study of the "ageing" of superconductors prepared in high oxygen pressure ($\mu$) and then subjected to oxygen outflux upon lowering of the pressure.

This work was supported by the Danish Natural Science Research Council under Grant Nos. J.nr. 5.21.99.72 and 11-7785, and the Danish Technical Research Council under Grant No. J.nr. 16-4296.K and 16-4750.K.

[1] J. D. Jorgensen, M. A. Beno, D. G. Hinks, L. Soderholm, K. J. Volin, R. L. Hitterman, J. D. Grace, I. K. Schuller, C. U. Segre, K. Zhang, and M. S. Kleefisch, Phys. Rev. B **36**, 3608 (1987).

[2] J. D. Jorgensen, B. W. Kwok, G. W. Crabtree, A. Umezawa, L. J. Nowicki, and A. P. Paulikas, Phys. Rev.

B **36**, 5731 (1987).
[3]G. Van Tendeloo, H. W. Zandbergen, and S. Amelinckx, Solid State Commun. **63**, 603 (1987).
[4]R. J. Cava, B. Batlogg, C. H. Chen, E. A. Rietman, S. M. Zahurak, and D. Werder, Nature (London) **329**, 423 (1987).
[5]S. I. Park, C. C. Tsuei, and K. N. Tu, Phys. Rev. B **37**, 2305 (1988).
[6]H. You, J. D. Axe, X. B. Kan, S. C. Moss, J. Z. Liu, and D. J. Lam, Phys. Rev. B **37**, 2301 (1988).
[7]N.-C. Yeh, K. N. Tu, S. I. Park, and C. C. Tsuei, Phys. Rev. B **38**, 7087 (1988).
[8]G. Ottaviani, C. Nobili, F. Nava, M. Affronfe, T. Manfredini, F. C. Matacotta, and E. Galli, Phys. Rev. B **39**, 9069 (1989).
[9]J. Li, S. Q. Wang, J. W. Mayer, and K. N. Lu, Phys. Rev. B **39**, 12 367 (1989).
[10]X. M. Xie, T. G. Chen, and Z. L. Wu, Phys. Rev. B **40**, 4549 (1989).
[11]R. Beyers, B. T. Ahn, G. Gorman, V. Y. Lee, S. S. P. Parkin, M. L. Ramirez, K. P. Roche, J. E. Vazques, T. M. Gür, and R. A. Huggins, Nature (London) **340**, 619 (1989).
[12]S. J. Rothman, J. L. Routbort, and J. E. Barker, Phys. Rev. B **40**, 8852 (1989).
[13]R. M. Fleming, L. F. Schneemeyer, P. K. Gallagher, B. Batlogg, L. W. Rupp, and J. V. Waszczak, Phys. Rev. B **37**, 7920 (1988).
[14]E. D. Specht, C. J. Sparks, A. G. Dhere, J. Brynestad, O. B. Cavin, D. M. Kroeger, and H. A. Oye, Phys. Rev. B **37**, 7426 (1988).
[15]A. G. Khachaturyan and J. W. Morris, Phys. Rev. Lett. **59**, 2776 (1987).
[16]J. M. Bell, Phys. Rev. B **37**, 541 (1988).
[17]L. T. Wille and D. de Fontaine, Phys. Rev. B **37**, 2227 (1988).
[18]L. T. Wille, A. Berera, and D. de Fontaine, Phys. Rev. Lett. **60**, 1065 (1988).
[19]A. G. Khachaturyan and J. W. Morris, Phys. Rev. Lett. **61**, 215 (1988).
[20]A. A. Aligia, A. G. Rojo, and B. R. Alascio, Phys. Rev. B **38**, 6604 (1988).
[21]Z.-X. Cai and S. D. Mahanti, Solid State Commun. **67**, 287 (1988).
[22]C. P. Burmester and L. T. Wille, Phys. Rev. B **40**, 8795 (1989).
[23]L. T. Wille, Phys. Rev. B **40**, 6931 (1989).
[24]Z.-X. Cai and S. D. Mahanti, Phys. Rev. B **40**, 6558 (1989).
[25]A. Berera and D. de Fontaine, Phys. Rev. B **39**, 6727 (1989).
[26]N. C. Bartelt, T. L. Einstein, and L. T. Wille, Phys. Rev. B **40**, 10 759 (1989).
[27]A. G. Khachaturyan and J. W. Morris, Phys. Rev. Lett. **64**, 76 (1990).
[28]D. de Fontaine, G. Ceder, and M. Asta, Nature (London) **342**, 544 (1990).
[29]T. Aukrust, M. A. Novotny, P. A. Rikvold, and D. P. Landau, Phys. Rev. B **41**, 8772 (1990).
[30]J. V. Andersen and O. G. Mouritsen (unpublished).
[31]We have also considered several situations of stepwise cooling which lead to results similar to those obtained for continuous cooling with the same overall cooling rate.
[32]R. F. Shannon, C. R. Harkless, and S. E. Nagler, Phys. Rev. B **38**, 9327 (1988).
[33]O. G. Mouritsen and P. J. Shah, Phys. Rev. B **40**, 11 445 (1989).